Investigation into the Dual Role of Shear Flow in 2D MHD Turbulence

Andrew P. L. Newton and Eun-jin Kim

Department of Applied Mathematics, University of Sheffield, Sheffield, S3 7RH, United Kingdom
(Received 22 October 2008; published 22 April 2009)

The turbulent diffusion η_T of a large-scale magnetic field B_0 is numerically studied in two-dimensional magnetohydrodynamic turbulence with an imposed shear flow. We demonstrate that a shear flow plays a dual role, quenching transport through shear destruction and enhancing it via resonance. Specifically without resonance $\eta_T \propto B_0^{-4}$ with no shear (rms shearing rate $= \Omega = 0$) and $\eta_T \propto \Omega^{-2.7}$ for $B_0 = 0$, while with resonance $\eta_T \propto B_0^{-2} \propto \Omega^{-2}$. These results indicate that the absence of resonance is responsible for the most catastrophic reductions in transport.

Fundamental processes governing the dynamics of coherent structures and their interplay with turbulence in magnetized fluids present some of the most outstanding problems in classical physics. In particular, various observations indicate that typical magnetic activities [e.g., solar magnetic cycles, solar flares, corona mass ejection (e.g., [1–3]) in astrophysical plasmas, saw-teeth, and major disruptions [4] in laboratory plasmas] must involve the fast transport of magnetic fields on time scales much shorter than the Ohmic diffusion time scale, which has challenged many previous authors. This is especially the case in single fluid magnetohydrodynamic (MHD) turbulence, where turbulent transport of magnetic fields is seriously quenched due to the backreaction of (small-scale) magnetic fields [2,5–7] even for a weak large-scale magnetic field far below equipartition.

Significant quenching in turbulent transport can also result from shearing by (stable) shear flows, which accelerate the forward cascade to small scales by eddy distortion or disruption, effectively enhancing the overall dissipation in a system [7–10]. While this shear quenching is vital for plasma confinement in laboratory plasmas (e.g., tokamaks, stellarators, etc. [10,11]), it adds more trouble to explaining the aforementioned fast magnetic activities. Thus the eminent question is whether or not the transport of magnetic fields is *super slow* under the influence of both magnetic back reaction and shear. In two-dimensional (2D) MHD, the turbulent dissipation rate η_T of magnetic fields in parallel with shear flows was indeed shown to be slowed down due to both effects [7]. The dependence of η_T on molecular Ohmic diffusivity η is, however, shown to be weaker $\propto \eta^{2/3}$ compared to η in the absence of shear flow. In two-fluid MHD, the dependence on η becomes even weaker ($\eta^{1/3}$) [12], suggesting a good possibility of fast magnetic dissipation (i.e., $\eta_T \propto \eta^0$) due to the decoupling of electrons from ions on fine scales.

In this Letter, we report on the first comprehensive direct numerical simulations of 2D (single fluid) sheared MHD turbulence to elucidate fundamental physical processes which accelerate or moderate transport. This is achieved by an extensive exploration of the parameter space, which previous analytical works [7,13] have been unable to investigate. We show that shear flows play an interesting *dual* role: quenching transport by shear distortion while simultaneously enhancing it via resonance [13,14]. In particular, a strong large-scale magnetic field $\mathbf{B}_0$ transforms turbulence eddies into packets of Alfvén waves of frequency $\omega_B = \mathbf{B}_0 \cdot \mathbf{k}$, with which the shear flow $\mathbf{U}_0$ can resonantly interact when Doppler shifted frequency $\omega_D = \omega - \mathbf{U}_0 \cdot \mathbf{k} = \pm \omega_B$. This leads to an enhancement of the turbulent diffusivity of $\mathbf{B}_0$, which would otherwise be severely quenched. Note that for effective transport, irreversibility through this resonance (and its overlap), stochasticity, and/or molecular dissipation is absolutely necessary. The results can have significant implications for understanding the role of waves and structures in turbulent transport in a variety systems (e.g., see [15]).

We consider incompressible MHD equations for the vorticity ($\omega = \nabla \times \mathbf{u}$) and magnetic vector potential A ($\mathbf{B} = \nabla \times A \hat{z}$) given in the dimensionless form:

$$[\partial_t + (\mathbf{U}_0 + \mathbf{u}) \cdot \nabla]\omega = \nu \nabla^2 \omega + \frac{1}{M^2}(\mathbf{B} \cdot \nabla)\nabla^2 A + F,$$

$$[\partial_t + (\mathbf{U}_0 + \mathbf{u}) \cdot \nabla]A = \eta \nabla^2 A. \quad (1)$$

Here, F is an external forcing; $\mathbf{U}_0$ is an imposed shear flow; $\mathbf{u}$ is the turbulent flow evolved consistently under the influence of $\mathbf{U}_0$ and the vorticity driving F; $M = v_c/v_A$ is the Alfvénic Mach number—the ratio of characteristic turbulent velocity v_c to the Alfvén speed v_A associated with a large-scale magnetic field; η and ν are molecular Ohmic diffusivity and viscosity which are assumed to be the same (i.e., magnetic Prandtl number $P_m = \nu/\eta = 1$). The forcing is chosen to have a power spectrum peaked around $|\mathbf{k}| \approx 5$, and temporally random with no characteristic frequency ($\omega_0 = 0$) and correlation time $\tau_C/2\pi = 1/\gamma$, thereby containing frequencies $\omega = \omega_0 \pm 2\pi/\tau_C = [-\gamma, \gamma]$. Here, γ is the decorrelation rate. As done in [5], we apply hyperviscosity on scales larger than that of the forcing to keep the characteristic wave number of turbulence $k \sim 5$ even in the kinematic limit (without inverse cascade or the formation of zonal flows).

We solve Eq. (1) by using spectral code with the 4th order accuracy (IFRK4) in a $(2\pi)^2$ box with periodic boundary conditions. The shear flow and initial large-scale magnetic field are chosen such that $\mathbf{U}_0 = \Omega \sin(x)\hat{y}$ and $\langle A(t=0)\rangle = A_0(t=0) = \cos x$ [$\mathbf{B}_0 = \nabla \times A_0\hat{z} = \sin(x)\hat{y}$], thus allowing no direct influence of shear on $\mathbf{B}_0$, i.e., $\mathbf{U}_0 \cdot \nabla\mathbf{B}_0 = 0$. Here, $\langle \rangle$ denotes an average over small-scale turbulence; Ω represents (maximum) shearing rate and velocity in our units. It is important to note that if $\mathbf{U}_0 \cdot \nabla\mathbf{B}_0 \neq 0$, $\mathbf{B}_0$ would be sheared and stretched directly by $\mathbf{U}_0$, thereby efficiently dissipated. We numerically determine $\eta_T = \langle u_x A\rangle/B_0$ from the decay rate of A_0, which is solely attributed to molecular (η) and turbulent diffusion for $\mathbf{U}_0 \cdot \nabla\mathbf{B}_0 = 0$. In the following, we present the results from three series of numerical simulations obtained by systematically varying M and Ω.

(i) Unsheared MHD.—We first perform simulations for the unsheared MHD turbulence ($\mathbf{U}_0 = 0$) by using $\tau_c = 1$ ($\gamma/2\pi = \tau_c^{-1} = 1$). At the beginning of the simulation, we see a slow decay of large-scale magnetic field A_0 due to the backreaction of small-scale magnetic fields (see also [5]). This slow mixing of A_0 is visually shown in Fig. 1(b), in comparison with Fig. 1(a) obtained without backreaction ($M \rightarrow \infty$). When A_0 becomes sufficiently weak with negligible backreactions, A_0 decays passively at a faster, kinematic turbulent diffusivity [see Fig. 1(a)] $\eta_K = \eta_T(B=0)$. The critical strength of magnetic fields for the suppression of η_T is found to be $M^2 = \eta_K/\eta$, in good agreement with [5]. Figure 2 shows the effective

magnetic Reynolds number $R_m = \eta_T/\eta$ as a function of $1/M^2 \propto B_0^2$ for $\eta = 0.0005$. Interestingly, two distinct regimes of different scalings with B_0 are identified. The first for $1 < M^2 < \eta_K/\eta$, $\eta_T \propto B_0^{-2.06}$, in agreement with [5]. However, for a very strong magnetic field $M < 1$, η_T decreases more rapidly with B_0, with the new scaling $\eta_T \propto B_0^{-4.04}$. The physical reason for these different scalings is resonance which occurs when $\omega = \pm\omega_B = \pm k \sin x/M$. Specifically, in the case when $M > k/2\pi(\sim 0.8)$, there always exists ω in the forcing frequency spectrum ($\omega/2\pi \in [-1, 1]$) which can resonate with some ω_B (i.e. for some x) mode, including the highest frequency $\sim k/M$ (near $x = \pi/2$ and $3\pi/2$) which has the strongest magnetic back-reaction. However, for $M < k/2\pi$, high frequency ($\sim k/M$) modes can no longer resonate, with the shrinking of the resonant width. Note that stochasticity ($\gamma \neq 0$) is crucial for a broad resonant layer, much wider than that due to classical dissipation.

To examine the effect of resonance in more detail, we take the Fourier transform of Eq. (1) with $\mathbf{U}_0 = 0$:

$$(i\omega + \epsilon)\tilde{A} = \tilde{u}_x B_0, \qquad (i\omega + \epsilon)\tilde{\omega} = i\omega_B k^2\tilde{A} + \tilde{F}. \quad (2)$$

The Fourier transform is denoted by $\sim$; $\omega_B = \mathbf{k} \cdot \mathbf{B}_0$ is the Alfvén frequency; ϵ involves both molecular dissipation ($\eta k^2 = \nu k^2$) and nonlinear damping. The solutions to Eq. (2) gives us $\eta_T = \langle u_x A\rangle/B_0$:

$$\eta_T \propto \frac{i}{B_0^2} \int d\omega(\omega + i\epsilon)\frac{2\omega_B}{(\omega + \omega_B)^2 + \epsilon^2}$$
$$\times \frac{2\omega_B}{(\omega - \omega_B)^2 + \epsilon^2}|F(\omega)|^2. \quad (3)$$

Here $|F(\omega)|^2$ is the frequency spectrum of the forcing. Note that the quasilinear result (3) is good for $\gamma \gg 1$ and/or weak turbulence (as in the case for strong shear and/or magnetic fields). To highlight the main point, we consider the following two extreme cases; (i) a short-correlated random forcing $|F(\omega)|^2 = 1/\gamma$ which contains all frequencies, always satisfying the resonance condition. (ii) a coherent wave forcing $|F(\omega)|^2 = \delta(\omega - \omega_*)$ with $\omega_* \ll \omega_B$, with no possibility of resonance. It is straightforward to see that in these two cases, Eq. (3) gives $\eta_T \propto 1/B_0^2\gamma$ and $\eta_T \propto \epsilon/B_0^4$, respectively. That is, resonance
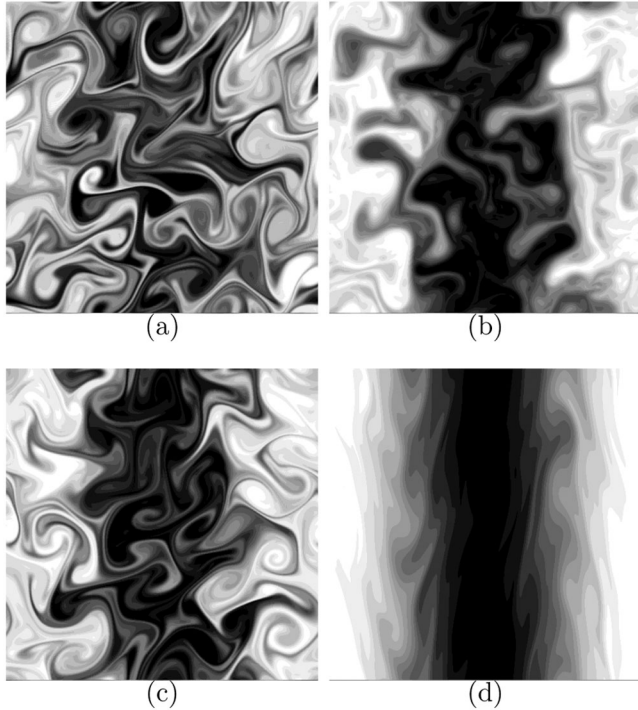

(a)   (b)

(c)   (d)

FIG. 1.   Diffusion (mixing) of A_0 for (a) $M^2 \rightarrow \infty(B_0 = 0)$ and $\Omega = 0$, (b) $M^2 = 10$ and $\Omega = 0$, (c) $M^2 \rightarrow \infty$ and $\Omega = 1.0$, and (d) $M^2 \rightarrow \infty$ and $\Omega = 10$. All are taken at $t = 5$ with $\tau_c = 1$.
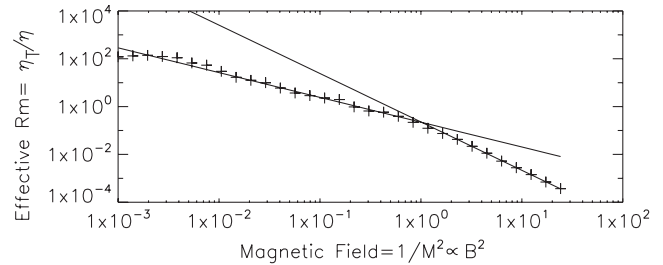

FIG. 2. $R_m = \eta_T/\eta$ vs $1/M^2$; lines represent the least square fits with scalings of $\eta_t \propto B_0^{-2.06}$ for weak ($M > 1$) and $\eta_T \propto B_0^{-4.04}$ strong magnetic field ($M < 1$) limits ($\Omega = 0$ and $\tau_c = 1$).

enhances transport, leading to a weaker dependence on B_0 as B_0^{-2}. Furthermore, for a wave forcing without resonance, not only η_T is significantly quenched, but also vanishes without finite dissipation ϵ as waves themselves cannot do any transport without dissipation. In this case, the turbulence is entirely made up of packets of Alfvén waves traveling along the magnetic field lines. It is the lack of resonant interplay between the magnetic field and turbulence which causes the catastrophic collapse of transport.

(ii) Sheared kinematic MHD.—To elucidate the effect of shear flows, we perform a set of experiments for sheared MHD turbulence in the kinematic limit, for no magnetic backreaction ($M \to \infty$). As before the turbulence is generated by forcing the vorticity on $k \sim 5$ wave numbers with $\tau_c = 1$. We first visually demonstrate that shear flow does quench magnetic transport in Fig. 1 by comparing the three cases: no shear $\Omega = 0$ (panel [a]), weak shear $\Omega = 1$ (panel [c]), and strong shear $\Omega = 10$ (panel [d]). In particular panel [d] shows the formation of a transport barrier (i.e. severe quenching in transport) perpendicular to the shear flow. The reduction in transport by shear flow is quantified in Fig. 3 where $R_m = \eta_T/\eta$ ($\eta = 0.005$) is plotted as a function of Ω for $\Omega \sim [0.001, 10]$. Note that R_m is related to the Lundquist number through $L = B_0 R_m/\Omega$. Of importance to notice is that the two different scalings with Ω are apparent, with the transition occurring when Ω is roughly comparable with turbulence decorrelation rate, i.e., $\tau_c = 1 \approx \Omega^{-1}$. That is, for weak shear $\Omega < 1$, η_T does not change much with Ω ($\eta_T \propto \Omega^0$) while for strong shear $\Omega > 1$, η_T rapidly decreases $\propto \Omega^{-2.7}$. Interestingly, the reason for this is twofold. First, note that for $U_0 = \Omega \sin x$, the resonance occurs locally when $\omega - \Omega k \sin x = 0$, where k (~ 5) is again the characteristic turbulence wave number. Thus, for $\Omega < k/2\pi$, there always exists $\omega/2\pi \sim [-1, 1]$ which satisfies the resonance condition (including the maximum U_0), thereby enhancing transport. This is similar to $M > k/2\pi$ case in (i) unsheared MHD, discussed earlier. Secondly, turbulence with $\tau_c < \Omega^{-1}$ changes its eddies too quickly to be subject to a coherent shearing effect. In comparison, for $\Omega \gg 1$, shearing becomes very efficient, significantly quenching η_T. That is, a shear flow leads to severe quenching when its shearing rate is the shortest time scale in the system.
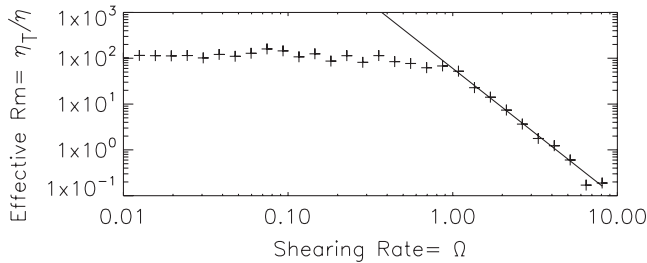
(iii) Sheared MHD.—The presence of magnetic fields and shear flows can introduce important new dynamics through the excitation of Alfvén waves which interact with shear flows and turbulence. One of the interesting consequences can be seen in Fig. 4 showing $R_m = \eta_T/\eta$ for $\eta = 0.001$ for different values of Ω and M with $\tau_c = 1$. When the magnetic field is sufficiently weak such that $M^2 > \eta_K/\eta$, η_T is unaffected by magnetic backreaction, recovering the unsheared kinematic result. For $1 < M^2 < \eta_K/\eta$, η_T is suppressed due to magnetic back reaction, similarly to the case without shear flow, discussed previously (see Fig. 2). However, for $M^2 < 1$, a considerable increase in η_T is noticeable around the resonant point due to the shear flow roughly when $\Omega \sim 1/M$ obtained by taking $\omega \sim 0$ in resonant condition $\omega - \Omega k \sin x \sim \pm k \sin x/M$. These resonant points are denoted by * in Fig. 4, with a good agreement between the location of these points and maximum transport, especially in the limit of strong magnetic field where the turbulence is almost Alfvénic. The resonance at this point is caused by the turbulent eddies being transported by $\mathbf{U}_0$ along the magnetic field lines at the Alfvén speed, which allows the Alfvén waves to be coherently forced, leading to the amplification of the amplitude of the Alfvén waves.

We obtain the scaling of the maximum value of η_T at resonant points as a function of B_0, by choosing the value of Ω satisfying the resonance condition. The results are shown in Fig. 5. In sharp contrast to Fig. 2 obtained with $\Omega = 0$, the scaling of $\eta_T \propto B_0^{-2}$ persists into the very strong magnetic field regime $M < 1$. This is because the shear flow shifts the frequency to match Alfvén frequency, leading to the resonant interaction between Alfvén waves associated with strong magnetic fields and turbulence, thereby averting the violent reduction of transport $\eta_T \propto B_0^{-4}$. This is an interesting result, highlighting another crucial effect of shear flow.

We demonstrate that these are robust results by performing similar simulations, but by using $\tau_c \to 0$ instead of $\tau_c = 1$. The results are plotted in Fig. 6. Immediately noticeable is the significant reduction in overall value of η_T compared to the case with $\tau_c = 1$ (see Fig. 4). This
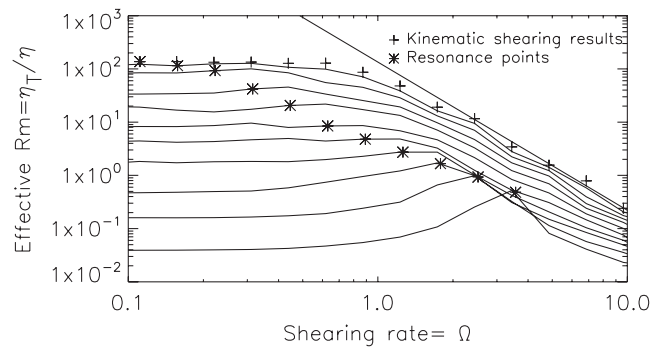
FIG. 3. R_m vs Ω, clearly showing the transition at $\Omega^{-1} = \tau_c = 1$ ($B_0 = 0$).

FIG. 4. R_m vs Ω for $\tau_c = 1$ and $1/M^2 \in [0, 0.01, \ldots, 10]$, with B_0 increasing from the top to the bottom. The symbol * approximately represents resonance point.
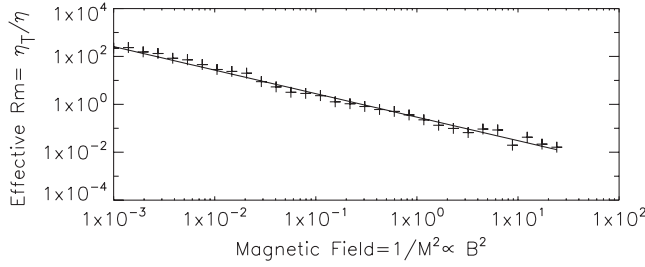
FIG. 5. R_m vs $1/M^2$ for $\tau_c = 1$ at resonant points for $(\omega - \Omega k \sim \omega_B)$. The line represents the least squares fit with the scaling $\eta_T \propto B_0^{-1.96}$.

FIG. 6. The same as in Fig. 4 but with $\tau_c \to 0$.

follows from $|F(\omega)|^2 \propto \gamma/(\omega_0^2 + \gamma^2) \to 1/\gamma$ for $\gamma \gg 1$ ($\tau_c \ll 1$). Furthermore, in the kinematic limit ($M \to \infty$), η_T is quenched $\propto \Omega^{-1}$ for strong shear, with a much weaker dependence on Ω compared to $\Omega^{-2.7}$ in the case of $\tau_c = 1$. This is because for $\tau_c \to 0$, the frequency of forcing can take any value, always satisfying the resonance condition $\omega - \Omega k \sin x = \pm k \sin x / M$ for all values of M and x. Note that this scaling is weaker than the theoretical prediction ($\eta_T \propto \Omega^{-2}$) given in [7] obtained by using an anisotropic forcing. The general tendency of weaker dependency on shear for the forcing with shorter correlation time is however generic, and is also found in previous works (see [7,13]). The increase of η_T at resonant points, marked by *, is also clearly seen in Fig. 6, which again shows the persistence of the scaling of $\eta_T \propto B_0^{-2}$ into $M^2 < 1$ due to resonances.

In summary, we have elucidated the key physical processes for transport, especially highlighting the indispensable role of coherent structures (magnetic fields and shear flows) in determining turbulent transport through the excitation of waves, shearing, and resonances [15]. In particular, we have demonstrated (i) that transport quenching by shear flows and resonant interactions is vitally important to understanding turbulence regulation in 2D MHD; (ii) that a shear flow plays a dual role of quenching transport by shearing, while enhancing it via resonance and the overlap of resonant layers; (iii) that a strong suppression of transport by shear flow (magnetic fields) occurs when the shearing (Alfvénic) time scale is shortest among all the characteristic time scales in the system (with no resonance between coherent structures, turbulence, and waves). Without resonance, $\eta_T \propto B_0^{-4}$ for weak shear and strong B_0, $\eta_T \propto \Omega^{-2.7}$ for strong shear and weak B_0; while with resonance $\eta_T \propto B_0^{-2} \propto \Omega^{-2}$ for both strong shear and B_0. These results were checked to be robust upon the change in the values of η and ν (across $\eta = \nu = 0.5, 1, 2, 4, 8 \times 10^{-3}$). We expect that similar results will hold for more general shear flows and equilibrium magnetic fields as long as they are stable.

Our results can have potentially significant implications for a variety of plasmas. Particularly, we expect similar physical p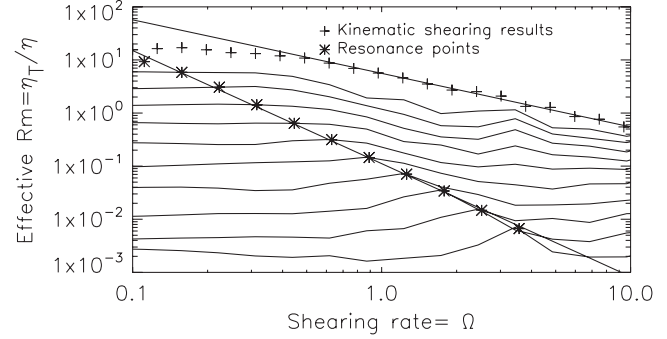rocesses for reducing or enhancing momentum transport and the alpha effect (in 3D MHD) [16], with a shear flow playing a similar dual role. This will have a crucial consequence in understanding the formation of self-generated zonal flows and dynamos, e.g., in astrophysical, space, and laboratory plasmas (the Sun, galaxies, tokamaks, RFP, etc.). Note that the formation of zonal flows does not take place in 2D MHD, and thus was not discussed in this Letter. Similar dual roles of shear flow will also be critical in understanding transport in other systems supporting waves (e.g., inertial waves in rotating fluids and gravity waves in stratified fluids). In MHD turbulence the shear quenching can, however, be weakened by the interference of magnetic field shear as shown in reduced 3D MHD [17]. These issues will be addressed in future papers.

[1] A. Choudhuri *et al.*, Phys. Rev. Lett. **98**, 131103 (2007).
[2] E. Kim and R. Diamond, Astrophys. J. **556**, 1052 (2001).
[3] P. Cassak *et al.*, Phys. Rev. Lett. **95**, 235002 (2005).
[4] B. B. Kadomsev, *Tokamak Plasma: A Complex Physical System* (Institute of Physics, London, 1992).
[5] F. Cattaneo and S. Vainstein, Astrophys. J. Lett. **376**, L21 (1991).
[6] A. Gruzinov and P. Diamond, Phys. Plasmas **3**, 1853 (1996).
[7] E. Kim and B. Dubrulle, Phys. Plasmas **8**, 813 (2001).
[8] K. H. Burrell, Phys. Plasmas **4**, 1499 (1997).
[9] E. Kim, Astron. Astrophys. **441**, 763 (2005).
[10] E. Kim, Mod. Phys. Lett. B **18**, 12 (2004).
[11] J. Boedo *et al.*, Phys. Rev. Lett. **84**, 2630 (2000).
[12] E. Kim, Phys. Rev. E **76**, 025401 (2007).
[13] J. Douglas *et al.*, Phys. Plasmas **15**, 052301 (2008).
[14] A. Newton and E. Kim, Phys. Plasmas **14**, 122306 (2007).
[15] P. Mininni and A. Pouquet, Phys. Rev. Lett. **99**, 254502 (2007).
[16] N. Leprovost and E. Kim, Phys. Rev. Lett. **100**, 144502 (2008).
[17] E. Kim, Phys. Plasmas **14**, 084502 (2007).